Chapter 3

The efficiency of heavy liquid separation to concentrate magnetic particles from pelagic sediments demonstrated by low-temperature magnetic measurements

Summary
Low-temperature rock magnetic measurements have distinct diagnostic value. However, in most bulk marine sediments the concentration of ferrimagnetic and antiferromagnetic minerals is that low, that even sensitive instrumentation often senses just the paramagnetic contribution of the silicate matrix in the residual field of the magnetometer. Analysis of magnetic extracts is usually performed to bypass the issue of low magnetic concentrations. Generally, magnetic extracts turn out to be not representative for the entire magnetic inventory. They are biased to components with high spontaneous magnetisation, such as magnetite and titanomagnetite being low coercive magnetic minerals. We show that high coercivity components are rather under-represented in such magnetic extracts. Additionally, classical magnetic extraction generally yields extracts that are coarser grained than the starting bulk sediment material. Therefore, making fully quantified inferences may not be warranted in any case. Here, we test as well heavy liquid separation, using hydrophilic sodium polytungsten solution $Na_6[H_2W_{12}O_{40}]$ and demonstrate its efficiency. Low-temperature cycling of zero-field-cooled, field-cooled and saturation isothermal remanent magnetisation acquired at room temperature were performed on dry bulk sediments, magnetic extracts, and heavy liquid separates, documenting the merit of the latter by showing much more detailed and representative low-temperature remanence measurements.

Key words: heavy liquid separation, magnetic extracts, marine sediments, Equatorial Atlantic Ocean, low-temperature magnetic measurements, Magnetic Properties Measurement System (MPMS)

This chapter is an article in review: Franke, C., Frederichs, T. and Dekkers, M.J., 2006. The efficiency of heavy liquid separation to concentrate magnetic particles from pelagic sediments demonstrated by low-temperature magnetic measurements, *Geophys. J. Int.*

1. Introduction

Rock magnetic investigations of marine sediments aim at unraveling depositional history and diagenetic changes of the magnetic mineralogy for geomagnetic and paleoceanographic investigations. As a rule in marine sediments, variably mixed magnetic components occur in very low concentration, down to the ppm range. In addition, the grain-size range of such particles spans from a few micrometers down to the nm range.

Clay minerals are the most abundant non-ferrimagnetic components in the sediment, besides carbonates and silica. They are important for a proper interpretation of low-temperature magnetic measurements of the bulk sediment, due to their paramagnetic behaviour. Because of their abundance, clay minerals may induce distinct magnetic moments even in the small residual fields prevailing in the magnetometer. Moreover, at temperatures below 25 K, paramagnetic (clay) minerals start to show collective magnetic behaviour that may give rise to appreciable magnetic moments (e.g. Coey 1988). Therefore, they attenuate diagnostic temperature transitions of proportional subordinate ferrimagnetic and antiferromagnetic mineral phases that occur only in trace amounts in almost all sediments. The expression of e.g. the

Verwey-, 34 K-, and Morin-transition of magnetite, pyrrhotite, and hematite respectively, is often below the limit of detection of the instrument used.

The standard tool to enhance the signal of the ferrimagnetic fraction is magnetic extraction. Various existing magnetic extraction techniques are known (e.g. Petersen *et al*. 1986; von Dobeneck 1987; Dekkers 1988; Hounslow & Maher 1999), whether or not combined by leaching the bulk sample material in acetic acid (pH 4 to 5) to dissolve the carbonates. These can be easily applied to wet bulk sediments of marine origin and yield a reasonable amount of extracted magnetic material, that subsequently can be analysed with a sensitive Magnetic Properties Measurement System (MPMS). Nevertheless, the amount of magnetic extract is generally still too low to allow a decent mass determination with a (semi-) microbalance ($d = 10^{-5}$ g). This expounds the problems of true quantification, required for budget calculations (Hounslow & Maher 1999). Comparisons of magnetic extract measurements with the bulk sediment signal, in order to determine how efficient and representative the extract is, are therefore not feasible in practice. Magnetic extraction methods favour strongly ferrimagnetic mineral phases (mainly (titano-) magnetite, maghemite, pyrrhotite and greigite), being magnetically softer, over magnetically harder antiferromagnetic phases (such as hematite or goethite) (Dekkers 1988; Hounslow & Maher 1999).

In this study, we applied heavy liquid separation on marine dry bulk sediments as an alternative extraction method, to achieve a more complete 'magnetic' extract, consisting of the heavy mineral fraction (density > 3.0 g cm^{-3}). This fraction includes all magnetic mineral phases being present in the sample. Hydrophilic sodium polytungsten solution $Na_6[H_2W_{12}O_{40}]$ was applied, providing the possibility to separate the magnetic fraction in very fine grained material, particular in clay-rich samples.

Watery lithium heteropolytungsten solution with a density of 2.85 g cm^{-3} was successfully used by Lagroix *et al.* (2004), to separate the magnetic Fe-Ti oxide fraction from the volcanic glass fraction in their tephra samples. This specific Old Crow tephra occurred intercalated in loess deposits at Halfway House in central Alaska. By classical gravity separation of 24 hours, they managed to divide the magnetic fraction into the lighter volcanic glass (< 2.85 g cm^{-3}) and the rest of the (coarser grained) magnetic Fe-Ti oxides (> 5.0 g cm^{-3}). They claim that their light mineral fraction additionally contains still most of the SP particles and the heavy fraction represents between 1.5 and 0.5% of the bulk sample mass. Certainly the density separation enhanced the possibilities to identify the Fe-Ti oxides in the heavy fraction, but concentrations in the light fraction were still high enough to magnetically identify its composition.The overwhelming amount of para-magnetic components in marine sediments complicates the separation and therefore hydrophilic sodium polytungsten solution with an even higher density of 3.0 g cm^{-3} was used in our study in combination with ultrasonic dispersion and centrifuging techniques to 'purify' the magnetic fraction from the siliceous components in the bulk sediment. The advantage of this non-magnetic separation method is that all magnetic components are extracted regardless their magnetic strength.

2. Sample Material

The chosen sample suite includes six specimens from clay-rich pelagic sediments of three gravity cores of a West-East profile throughout the Equatorial Atlantic. The gravity cores were recovered from the Ceará Rise (GeoB 1523-1, 3°50.8'N and 41°36.6'W), the equatorial Mid-Atlantic Ridge (GeoB 4313-2, 4°02.8'N and 33°26.3'W) and the Sierra Leone Rise (GeoB 2910-1, 4°50.7'N and 21°03.2'W) during *RV Meteor* cruises M16/2, M29/3 and M38/1. This zone in the Equatorial Atlantic is presently oligotrophic (Funk *et al.* 2004b). The pelagic sediments of all

three gravity cores are characterised as clay- and foram-bearing nannofossil oozes. Magnetic particles in these sediments originate from several distinct sources: continental eolian dust (Sahara), fluvial discharge (Amazon River) and submarine weathered ocean ridge basalts (Mid-Atlantic Ridge). Authigenic sources for magnetic particle input constitute the biogenic formation of bacterial magnetosomes and the (inorganic) recrystallisation of previous iron sulphides (Franke *et al*. unpublished data). For further details on gravity core localities and general settings see also Schulz *et al*. (1991), Henrich *et al.* (1994), Fischer *et al*. (1998), Funk *et al*. (2004a, 2004b), and Reitz *et al*. (2004).

Two discrete samples were processed from each of the three gravity cores, one corresponding to Marine Isotope Stage (MIS) 4, i.e. a glacial stage and the other to MIS 5.5 (Eemian), an interglacial stage. These samples, chosen for the detailed studies, represent typical conditions throughout the gravity cores. In glacial conditions a coarser magnetic inventory was found, while interglacial conditions are characterised by a finer magnetic grain-size distributions (Funk *et al*. 2004a, 2004b; Franke *et al.* unpublished data) so the magnetic upgrading procedures can be assessed for contrasting climatic conditions.

3. Upgrading Procedures

3.1 Magnetic Extraction

Magnetic extraction was performed on 10 cm³ of the wet bulk sediment samples using the method of Petersen *et al.* (1986). After the extraction run (8 to 12 hours per sample) the extracted particles were stored in small glass vials filled with ethanol. For MPMS measurements the fluid (containing the magnetic extract) was applied into a gelatine capsule and the sample was dried at room temperature, by evaporating the ethanol in air. Mass determination with a semi-microbalance was not possible, since the typical amount of a magnetic extract is beyond the metering precision of a semi-microbalance ($d = 10^{-5}$ g). Other, more detailed MPMS sample preparation aspects and instrumental settings are outlined in Frederichs *et al.* (2003).

3.2 Heavy Liquid Separation

Heavy liquid separation was performed on typically 0.8 g of the freeze-dried bulk sediments (referred to as dry bulk sediment). After weighing, the samples were dispersed (manually shaking until no obvious clustering was visible anymore, followed by 10 min of ultrasonic bath agitation) in 20 ml hydrophilic sodium polytungsten solution $Na_6[H_2W_{12}O_{40}]$, with a density of exactly 3.0 g cm^{-3}. The 50 ml plastic centrifuge vessels, containing the sediment-fluid suspension, were hereafter directly centrifuged for 5 min using a *Heraeus Minifuge T* at 4000 rps. During this process, the sediment-fluid suspension separates into a floating light sediment fraction (LF) with a density < 3.0 g cm^{-3}, the so-called fluid mirror (= 3.0 g cm^{-3}) in the middle of the centrifuge tube and a heavy sediment fraction (HF) at the bottom, with a density > 3.0 g cm^{-3}. If necessary, the 5 min centrifuge run was repeated without re-homogenising the sample. The LF on top of the fluid mirror and the fluid mirror itself were separated from the HF using a special 10 ml precision pipette, and both fractions were suction filtered separately after separation. For filtration, cellulose acetate filters with 0.1 µm pores were applied. The sediment fractions were dried in air over night (at room temperature), removed from the filters, weighed and filled in gelatine capsules for MPMS measurements.

3.3 Extraction Efficiency

In Table 1, the mass of the starting material of the dry bulk sediment is given, in comparison with the mass of the light and heavy fractions resulting from the density separation. The separated heavy mineral fraction for this sample set ranged from 0.022 to 0.004 g (Table 1), typically 1.4 % of the starting bulk material. The discrepancy between starting material and the sum of light and heavy fractions therefore

Table 1. Heavy liquid separation: masses of starting material, resulting light and heavy fraction, and the material on the filters. The upgrading factor was calculated as the ratio of the mass specific remanences (σ_r) of heavy fraction (HF) to dry bulk sediment (BS) at 300 K, $\frac{\sigma_{r,\,HF\;300K}}{\sigma_{r,\,BS\;300K}}$

Sample	Mass of Starting Material [g]	Total Mass Light Fraction [g]	Rel. Mass Light Fraction [%]	Total Mass Heavy Fraction [g]	Rel. Mass Heavy Fraction [%]	Material on Filters [g]	Material on Filters [%]	Upgrading Factor [ ]
GeoB 1523-1, 160 cm	0.85575	0.81556	95.3	0.0050	0.6	0.0351	4.1	16.3
GeoB 1523-1, 311 cm	0.65728	0.59048	89.8	0.0092	1.4	0.0576	8.6	18.6
GeoB 4313-2, 130 cm	0.68251	0.61931	90.7	0.0096	1.4	0.0536	7.9	14.4
GeoB 4313-2, 245 cm	0.79249	0.70829	89.4	0.0221	2.8	0.0621	7.9	5.2
GeoB 2910-1, 60 cm	0.97421	0.90021	92.4	0.0041	0.4	0.0699	7.2	12.9
GeoB 2910-1, 141 cm	0.87386	0.78406	89.7	0.0145	1.7	0.0753	8.6	11.6

Table 2. Masses of the dry bulk sediment, light and heavy fraction samples used for thermomagnetic measurements. These masses were applied for mass specific normalisation. Measurements on dry bulk sediment were performed on identical material with sample masses given in the second column. Note that only a minor portion of the light fraction was used for MPMS measurements.

Sample	Mass Dry Bulk Sediment [g]	Mass Light Fraction [g]	Mass Heavy Fraction [g]
GeoB 1523-1, 160 cm	0.03153	0.0625	0.0050
GeoB 1523-1, 311 cm	0.02663	0.0609	0.0092
GeoB 4313-2, 130 cm	0.02806	0.0510	0.0096
GeoB 4313-2, 245 cm	0.03429	0.0288	0.0221
GeoB 2910-1, 60 cm	0.02902	0.0491	0.0041
GeoB 2910-1, 141 cm	0.03446	0.0475	0.0145

stems from remaining material on the filters and can be further estimated by weighing the empty and remaining filters after removal of the separated density fractions. The amount of remaining material on the filters is comparable for both density fractions, typically 7.4 %. The amount of magnetic extracts for the same sample set using a much higher amount of starting material (10 cm^3 of wet bulk sediment) results in much lower yields, which cannot be meaningfully mass quantified. In the remainder, all thermomagnetic curves are mass normalised (Table 2), of course except the magnetic extract measurements. An additional advantage of the sodium polytungsten solution as used heavy liquid solution is its non-toxicity. Moreover, the separates can be flushed or washed extensively during filtration, due to the hydrophile character of the sodium polytungsten solution. The upgrading factor of the heavy liquid separation can be quantified in average to 13.2 (Table 1) and allows for control measurements for extraction results of the light and heavy fraction.

4. Thermomagnetic Observations

4.1 Thermomagnetic Measurements

Low-temperature zero-field-cooled (ZFC) and field-cooled (FC) measurements were performed within several weeks after drying the various extracts and separates, using a *Quantum Design XL7 Magnetic Properties Measurement System* (MPMS; noise level ~10^{-11} Am^2), applying a 5 T field at 5 K (for dry bulk sediments at 10 K). Low-temperature warming curves (5 to 300 K) were determined for dry bulk sediments, magnetic extracts, and heavy liquid separates monitored in 2 K increments. For the ZFC measurements, the field was applied at 5 K and was switched off before warming back to 300 K, whereas for the FC measurements, the field was applied at 300 K throughout cooling and switched off before warming back to 300 K. Where appropriate, the first derivatives of both ZFC and FC remanences vs. temperature were cal-culated (in 6 K average value = 3 data points) in order to better visualise changes of the magnetic state during sample warming.

To test for the presence of high coercivity components in the samples (see section 4.3), specific heating experiments were performed. First of all, the pristine dry bulk sediment samples were heated in air up to 340°C. Afterwards, the same procedure for low-temperature ZFC and FC runs in the MPMS was performed on the accordingly heated bulk sediments. The pristine and the heated bulk sediment samples were weighted before performing the low-temperature measurements, therefore the curves are normalised on their respective sample mass and thus the results are directly comparable.

For identification of the high coercivity component(s), additional high-temperature field cycling in the MPMS was performed on the dry bulk sediment samples, applying a 7 T field at room temperature. The samples were run in-field (FH) from 300 to 400 K (heating) and back to room temperature (cooling), followed by a zero-field (ZFH) cycle within the same temperature range. All high-temperature measurements using the MPMS were monitored in 2 K increments. FH curves are corrected for the paramagnetic contribution, which was derived from the linear slope of high-field dependence measured at room temperature between 4 and 7 T.

The room temperature saturation isothermal remanent magnetisation (RT-SIRM) measurements for dry bulk sediments, magnetic extracts, and heavy liquid separates were performed using a 5 T field (applied at RT), before the respective sample was cycled from 300 to 5 K (cooling) and back to room temperature (warming) in zero-field, monitored in 2 K increments.

4.2 Low-Temperature ZFC and FC Results of Dry Bulk Sediments

For all dry bulk sediment measurements, the low-temperature warming curves of ZFC and FC remanence did not show any pronounced remanence transitions (Fig. 1). A rapid decrease in ZFC and FC rema-

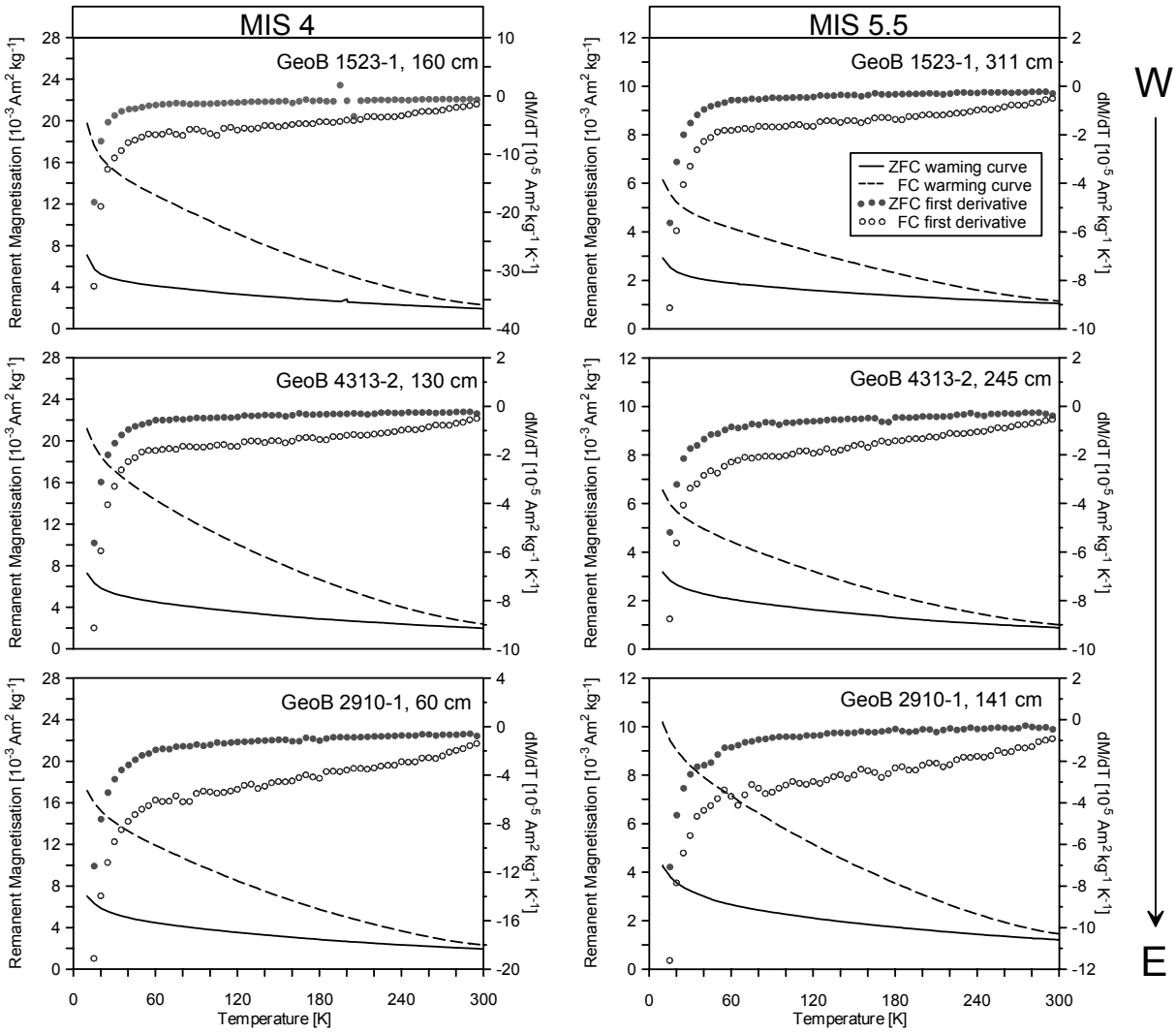

Figure 1. Low-temperature ZFC and FC remanent magnetisation curves for six dry bulk sediment samples (solid line = ZFC, dashed line = FC) along the Equatorial Atlantic West-East profile (from top to bottom). The magnetically coarser samples from glacial stage MIS 4 are shown on the left (scaled to a maximum value of $28 \cdot 10^{-3}$ Am^2 kg^{-1}) and the magnetically finer samples from interglacial stage MIS 5.5 are shown on the right (scaled to a maximum value of $12 \cdot 10^{-3}$ Am^2 kg^{-1}). ZFC and FC warming curves (applied field 5 T) were monitored from 10 to 300 K in 2 K increments. The first derivatives are given in gray, filled symbols for ZFC and open symbols for FC. No evident low-temperature features, such as the Verwey transition, were identified in the dry bulk sediment measurements. All curves are normalised to their respective sample mass.

nence between 10 and 40 K (corresponding to the local minimum in the respective first derivative curves) was observed for all six samples. A similar phenomenon was observed in partially oxidised magnetite of synthetic origin (Özdemir *et al*. 1993) or natural origin (Smirnov & Tarduno 2000). In the latter co-existing ultrafine-grained super-paramagnetic (SP) material is argued to occur. Passier & Dekkers (2002) discussed the possibilities of magnetic interaction, surface effects in very fine grains, or the presence of surface layers around coarser magnetic particles as other possible explanations for such behaviour.

The most important observation of all dry bulk sediment experiments was the remarkable discrepancy between corresponding ZFC and FC curves. These divergences are maximum at 10 K and disappear towards room temperature (Smirnov & Tarduno 2000). Divergences are generally bigger in samples from MIS 4 than in samples from MIS 5.5.

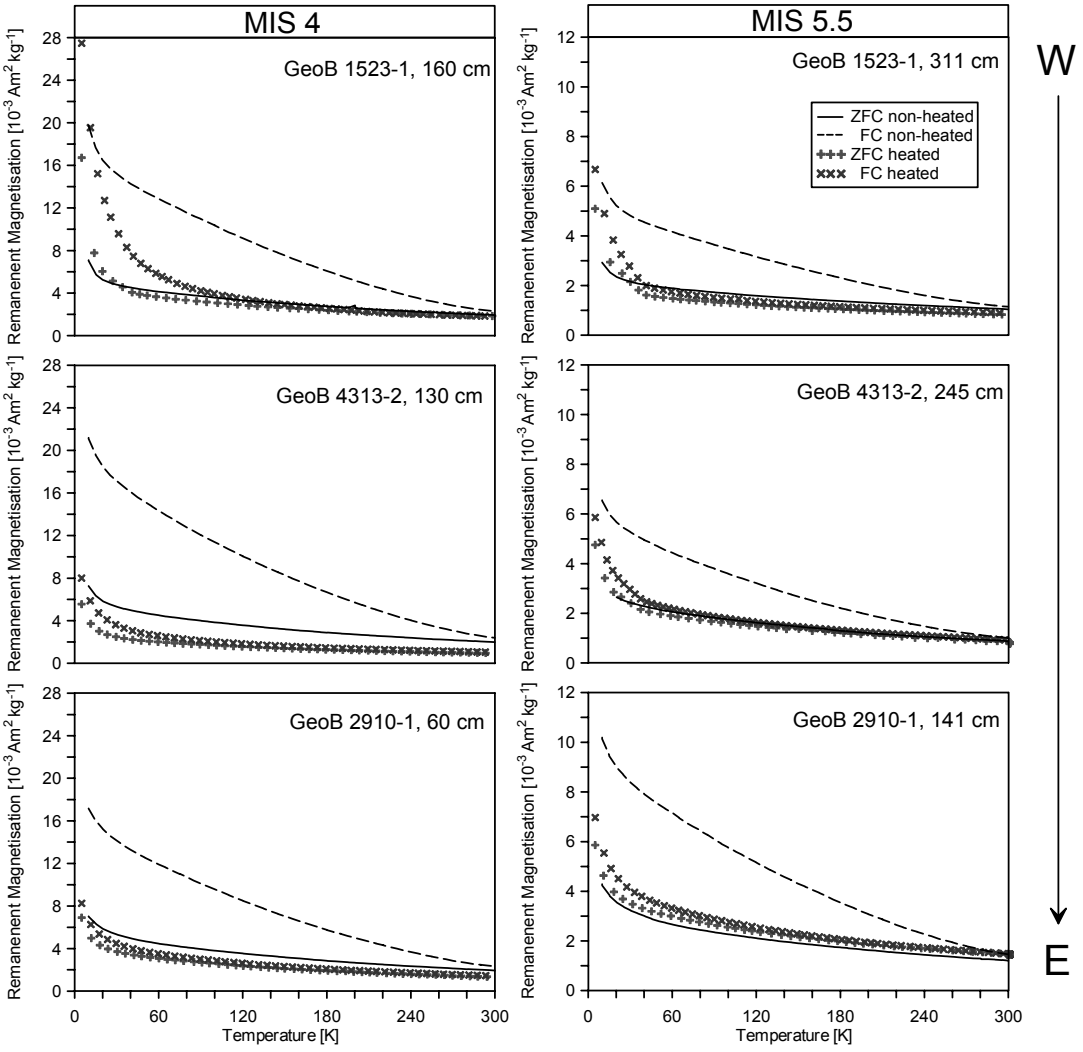

Figure 2. Low-temperature ZFC and FC remanent magnetisation curves for six pristine dry bulk sediment samples (solid line = ZFC, dashed line = FC) from West to East (from top to bottom) in comparison with the cross symbols, which refer to dry bulk sediments previously heated to 340°C; cross symbols for ZFC warming, x-symbols for FC warming curves. Samples from MIS 4 are shown on the left, samples from MIS 5.5 are shown on the right (for scaling compare Fig. 1). ZFC and FC warming curves of the pristine dry bulk sediment were measured from 10 to 300 K in 2 K increments, using an applied field of 5 T, whereas low-temperature ZFC and FC warming curves of the previously heated samples were monitored from 5 to 300 K in 2 K increments, also using an applied field of 5 T. Note the very slight offset at ~300 K of the heated bulk sediment set of curves, which is assumed to originate from an instrumental offset, it can be disregarded here. All curves are normalised to their respective sample mass.

4.3 Heating Experiments of Dry Bulk Sediments

The hypothesis of the presence of goethite was tested by the heating experiments outlined in section 4.1. The discrepancy between ZFC and FC curves decreased dramatically after heating and for most of the samples, ZFC and FC curves merge at temperatures higher than 40 to 60 K (compare Fig. 1 with Fig. 2). The decrease of the low-temperature ZFC-FC divergence after heating to 340°C is interpreted as the absence of the initial goethite signal contribution. This high coercivity component was chemically altered by heating above its Néel point of ~120°C (Dekkers 1989; France & Oldfield 2000; Özdemir & Dunlop 2000).

Further high-temperature remanence measurements (see 4.1) were performed to confirm this interpretation and check for the possibility of thin maghemitised surface layers of magnetite grains (van Velzen & Zijderveld 1992, 1995; van

Velzen & Dekkers 1999a, 1999b). All ZFH and FH curves and their first derivatives(Figs 3 and 4) show a drop at 390 K (~117°C), indicating the Néel point of goethite (e.g. Hedley 1971, Dekkers 1989). During cooling of the ZFH curves (Fig. 3) no new remanence was picked up by the samples, due to the lack of an inducing field. The minor remanence acquisition in some the ZFH cooling curves is caused by a small remaining field (in the order of±150 µT), which is still

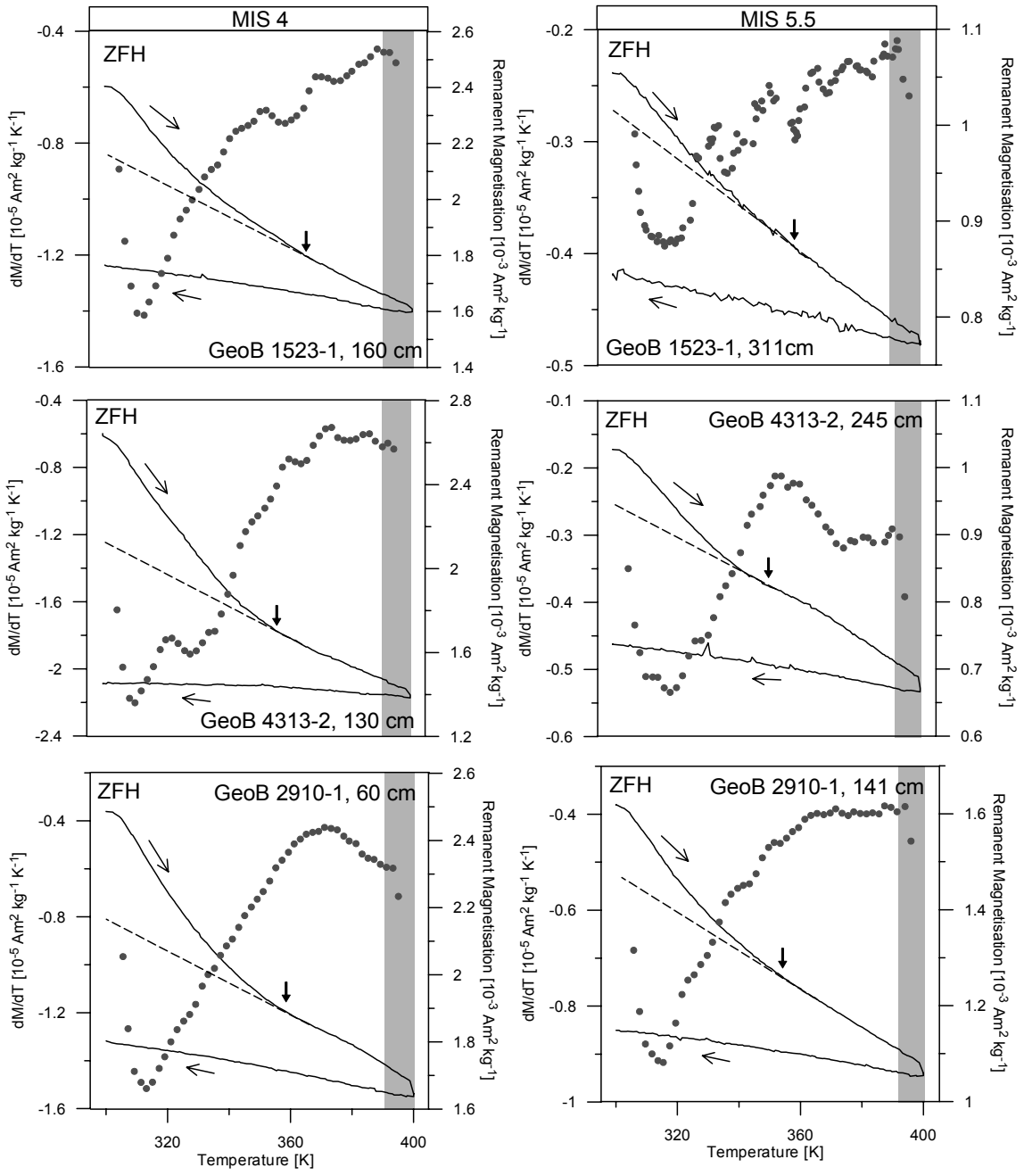

Figure 3. High-temperature cycling of the dry bulk sediments in zero-field (ZFH, solid line), using an applied field of 7 T at 300 K, which was switched off during heating and cooling between 300 and 400 K. The ZFH heating curves show a continuous decrease in remanence, gray shaded areas mark the sharp drop in remanence at 390 to 395 K. Filled symbols show the first derivative of the ZFH heating curve. Note that the ZFH cycle was performed after the FH cycle (compare Fig. 4). All curves are normalised to their respective sample mass. The magnetic non-goethite amount are established by linear extrapolation (dashed lines, after Dekkers 1989) of the decay curve from temperatures above the bending point (vertical bold arrows).

present after the quenching of the MPMS magnet (Kosterov *et al*. 2006).The FH heating curves show a characteristic Hopkinson peak at 360 K (~87°C, e.g. Heller 1978) for most of the samples (Fig. 4).

This feature is even more noticeable in the first derivative curves of the FH of

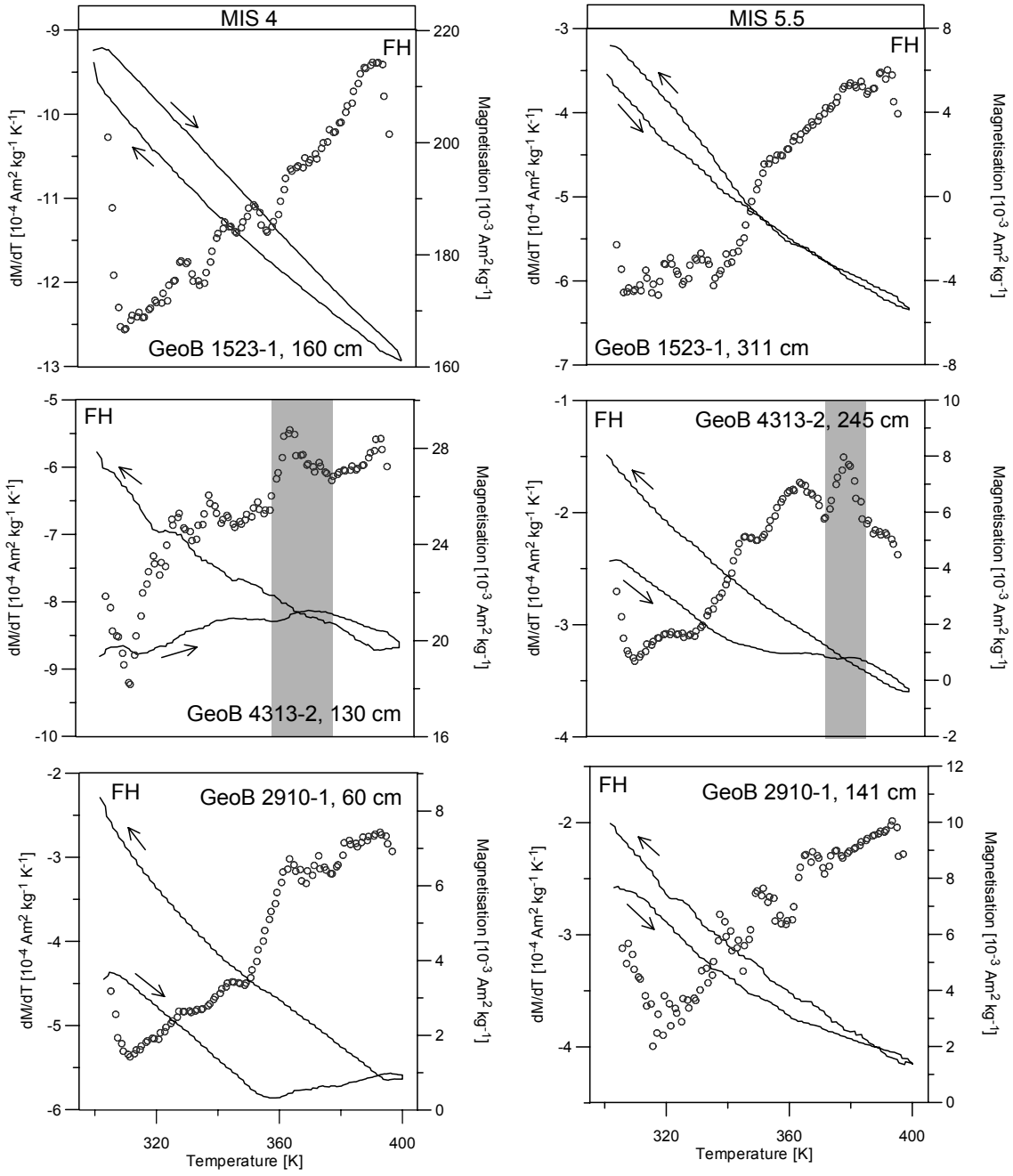

Figure 4. High-temperature cycling of induced magnetisation of pristine dry bulk sediments between 300 and 400 K in an applied field of 7 T (FH, solid line). The FH magnetisation curves were monitored in 2 K increments and are corrected for the paramagnetic contribution. According to the Curie-Weiss-Law, the paramagnetic contribution is assumed to be dependent on 1/T absolute and was achieved by field-depending measurements of the dry bulk sediments between 4 and 7 T at room temperature (not shown here). Open symbols show the first derivatives of the FH heating curves. Grey shaded areas indicate the position of the Hopkinson peak in FH heating curves between 370 and 380 K in samples from core GeoB 4313-2. Cooling curves of the FH measurements show an increase in induced magnetisation at room temperature, except for sample GeoB 1523-1, 160 cm. All curves are normalised to their respective sample mass.

samples from GeoB 4313-2. Note that the intensities of the samples increase after heating above the Néel point of goethite. This is a further indication that indeed most likely a reasonably moderate goethite component is present in these samples.

4.4 Low-Temperature ZFC and FC Results of Magnetic Extracts

The ZFC and FC warming curves for the magnetic extracts (Fig. 5) show four orders of magnitude lower remanence intensities (10^{-7} Am²) than the dry bulk sediments (10^{-4} Am²). Due to the low amount of magnetic extract, the curves (both ZFC and FC) have been simply normalised to the ZFC value at 5 K. The ZFC and FC curves depict a slightly broadened Verwey transition at ~110 K for the samples from the westernmost and the central equatorial sediment cores (GeoB 1523-1 and GeoB 4313-2). No Verwey transition could be observed for GeoB 2910-1, the easternmost site. The shift to slightly lower transition temperatures is indicative of non-stoichiometric slightly oxidised magnetite (Özdemir *et al.* 1993; Kosterov 2003).

The evident discrepancy between ZFC and FC warming curves in the dry bulk sediments was not observed in the magnetic extract data (compare Fig. 1 with Fig. 5). ZFC and FC warming curves of the magnetic extracts diverge only between 5 and 30 K. They are more or less merged at temperatures from ~110 K up to room temperature (see also Smirnov & Tarduno 2000). The substantially reduced ZFC-FC divergence in the magnetic extracts as compared to the bulk material would comply with the (near) absence of goethite in the magnetic extracts, because magnetic separation is biased towards strongly magnetic low coercivity material.

4.5 Low-Temperature ZFC and FC Results of Heavy Liquid Separates

Low-temperature warming curves of ZFC and FC remanence of the separated heavy fraction are overall an order of magnitude higher in intensity than those of the dry bulk sediments (Fig. 6). They show a very distinct steep slope between 5 and 40 K, corresponding to the sharp change of slope in the respective first derivatives. This might be due to the presence of an ultrafine-grained superparamagnetic (SP) phase (Özdemir *et al*. 1993; Smirnov & Tarduno 2000). The Verwey transition at ~110 K was exclusively detected in the westernmost samples of core GeoB 1523-1, it is weakly expressed in the first derivatives of the corresponding ZFC and FC curves.

The discrepancy between ZFC and FC curves mentioned earlier, which is interpreted to be caused by the presence of goethite, is clearly developed in the heavy fractions as compared to the magnetic extracts (compare Fig. 5 and Fig. 6). However, the discrepancy is less strong than in the dry bulk sediment samples. Therefore, the high coercitivity fraction is at least partly successfully extracted during the heavy liquid separation. The significant presence of the high coercivity component might also be the reason for the blurring of the Verwey transition earlier detected in the Mid Atlantic Ridge samples. The heavy liquid separation is not biased for magnetite in comparison to titanomagnetite or goethite, thus the curves of the heavy fraction represent the entire proportion of the magnetic assemblage. The ZFC and FC warming behaviour of the light fractions does not show any characteristic features and is therefore not shown here.

4.6 RT-SIRM Cycling Results

Dry Bulk Sediments compared with Heavy Liquid Separates

Figure 7 shows the RT-SIRM curves of the bulk sediment samples compared to the heavy (HF) and light fraction (LF) derived from heavy liquid separation. The cooling curves of the dry bulk sediments show a gradual increase of remanence from RT down to 10 K for all samples, which is distinctly enhanced below 10 K for most of the samples. On warming, the curves resemble the corresponding cooling curves back to ~150 K. Above 150 K the warming curves proceed below the cooling curves.

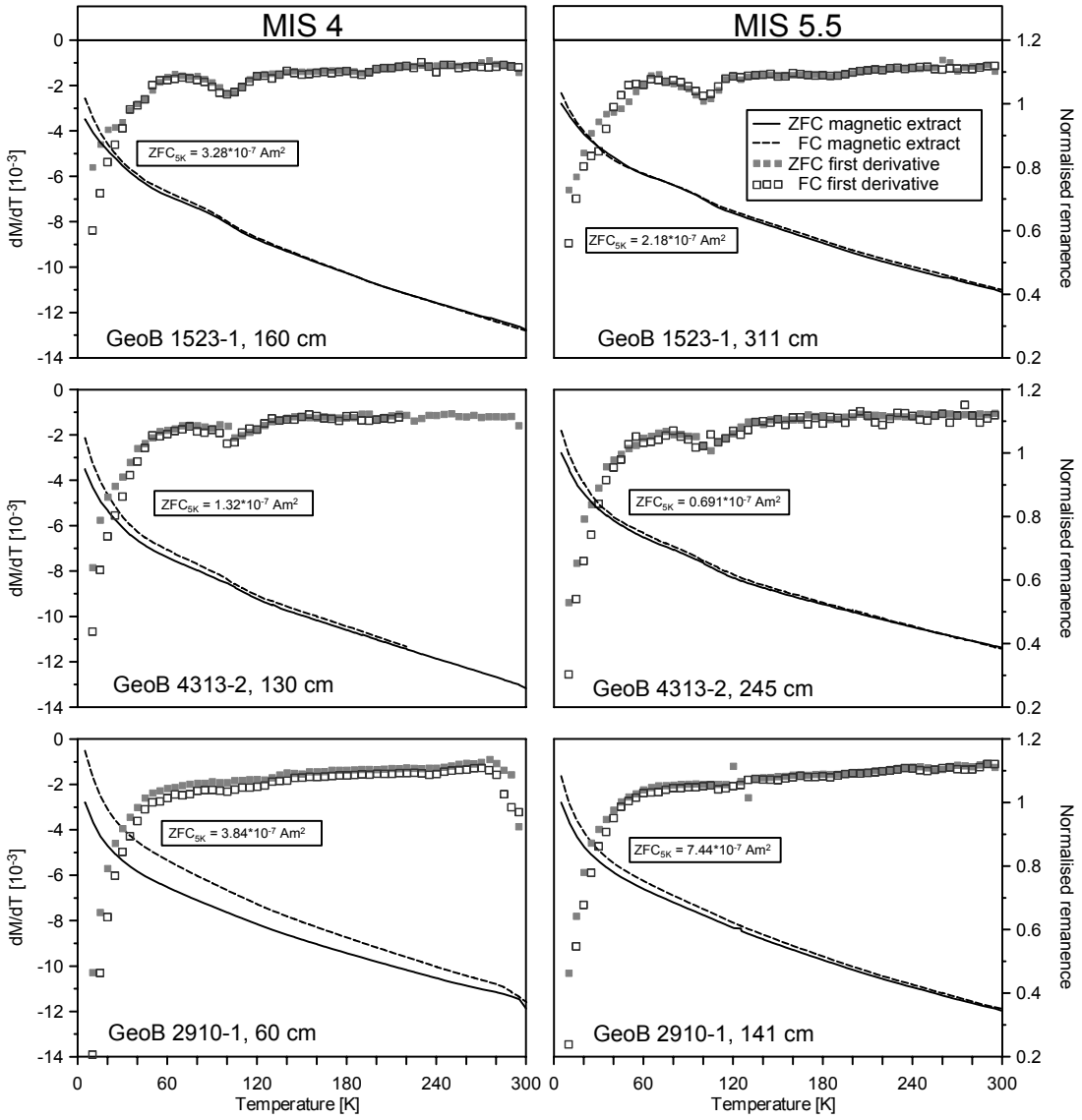

Figure 5. Low-temperature ZFC and FC remanence warming curves for magnetic extracts of all six samples from a West to East profile (from top to bottom).Lines refer to the ZFC and FC warming curves of the magnetic extract (solid line = ZFC, dashed line = FC) between 5 and 300 K in 2 K increments, using an applied field of 5 T. Curves are normalised to the magnitude of the respective ZFC value at 5 K (given for each individual panel). Because of very low yields normalising by mass was not practical in case of the magnetic extracts. Gray squares refer to the first derivatives of the respectively remanence curves (filled symbols = slope of ZFC, open symbols = slope of FC). For samples from GeoB 1523-1, a slightly shifted Verwey transition was detected at ~110 K, which can be also observed in samples from GeoB 4313-2, but is much weaker expressed at this site. No Verwey transition was found for samples of GeoB 2910-1. All ZFC and FC curves have the same ordinate scale.

No specific magnetic transitions were noted in the dry bulk sediment measurements.

The remarkable increase in remanence occurring in the very low temperature range between 10 and 5 K can also be observed in the room temperature SIRM curves of the light fraction (LF). Therefore it is most likely due to low-temperature magnetic ordering of paramagnetic (clay-) minerals (Coey 1988). Because the residual field of the MPMS is very low, this low-temperature ordering of the clay minerals in zero-field could be caused by the SIRM residing in magnetic mineral phases. This would magnetically couple to e.g. clay mineral coatings or ferrihydrite in the direct vicinity of the magnetic particles. Additional transmission electron microscopic (TEM) investigations of the samples

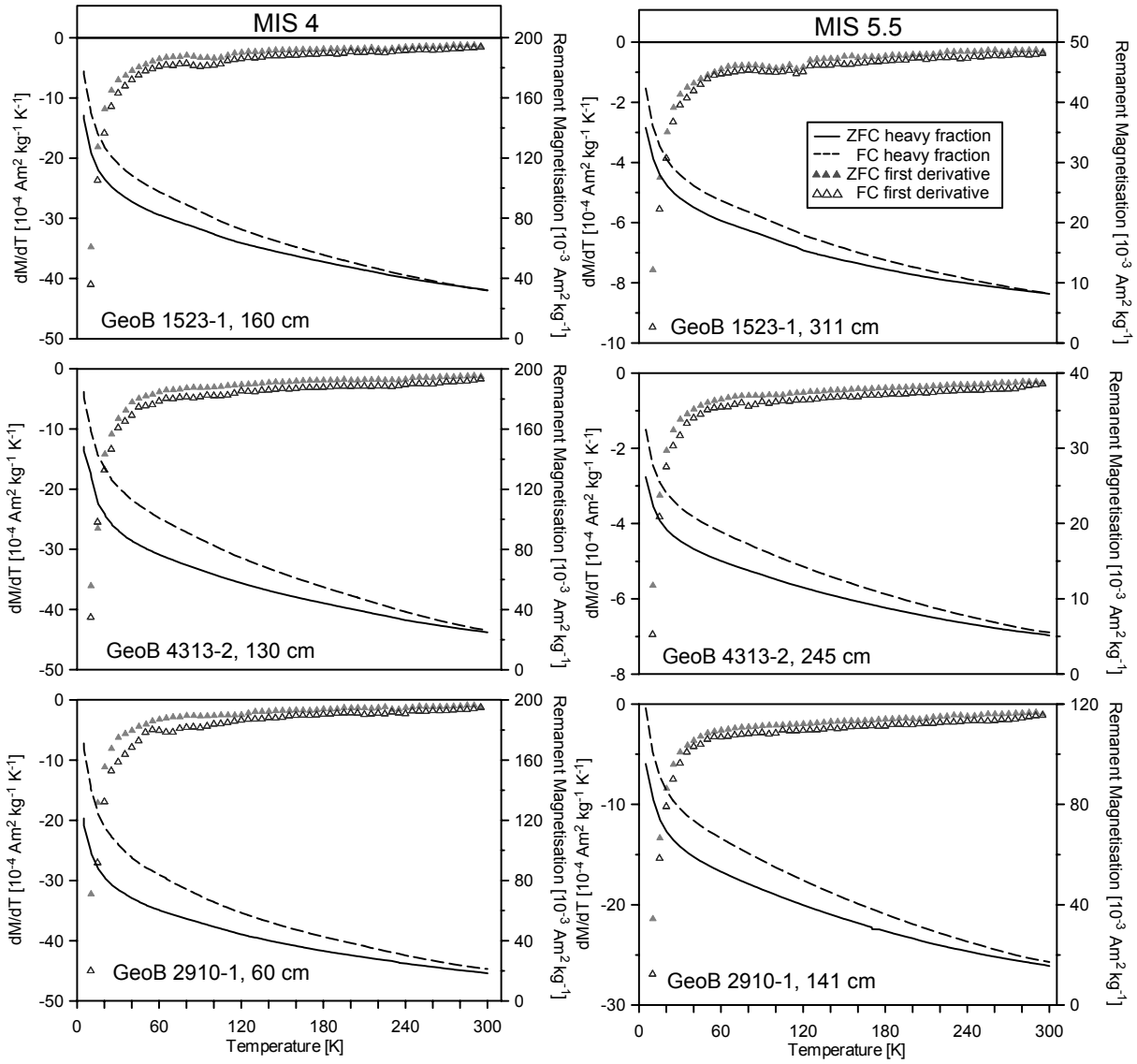

Figure 6. Low-temperature ZFC and FC remanence warming curves for the heavy fractions of the heavy liquid separates of the six samples from a West to East profile (from top to bottom). Lines refer to the ZFC and FC warming curves of the heavy fraction (solid line = ZFC, dashed line = FC), monitored between 5 and 300 K in 2 K increments, using an applied field of 5 T. Gray triangles refer to the first derivative of the respective remanence curves (filled symbols = slope of ZFC, open symbols = slope of FC). For samples from GeoB 1523-1, a weakly expressed Verwey transition was detected at ~110 K. All curves are normalised to their respective sample mass.

support the presence of such suggested mineral phases (Franke *et al*. unpubl. data). On the other hand, this would also suggest that the LF still contains part of the very fine grained SP fraction.

Usually LF curves are quite similar to the dry bulk sediment curves in sense of their general shape and increasing behaviour at very low temperatures. No specific magnetic transitions were detected in the LF measurements. Generally, they show a less steep slope towards lower temperatures and a weaker total intensity. This seems to be reasonable, because the heavy magnetic minerals are present in the HF (and of course in the dry bulk sediments), whereas the LF should be dominated by the lighter non-magnetic mineral fraction, such as clays, silicates, carbonates etc.

If the separation was successful to 100%, the LF would not carry any magnetic remanence and therefore would show a purely paramagnetic low-temperature curve. In practice, the separation seems to be quite efficient, but not abso-

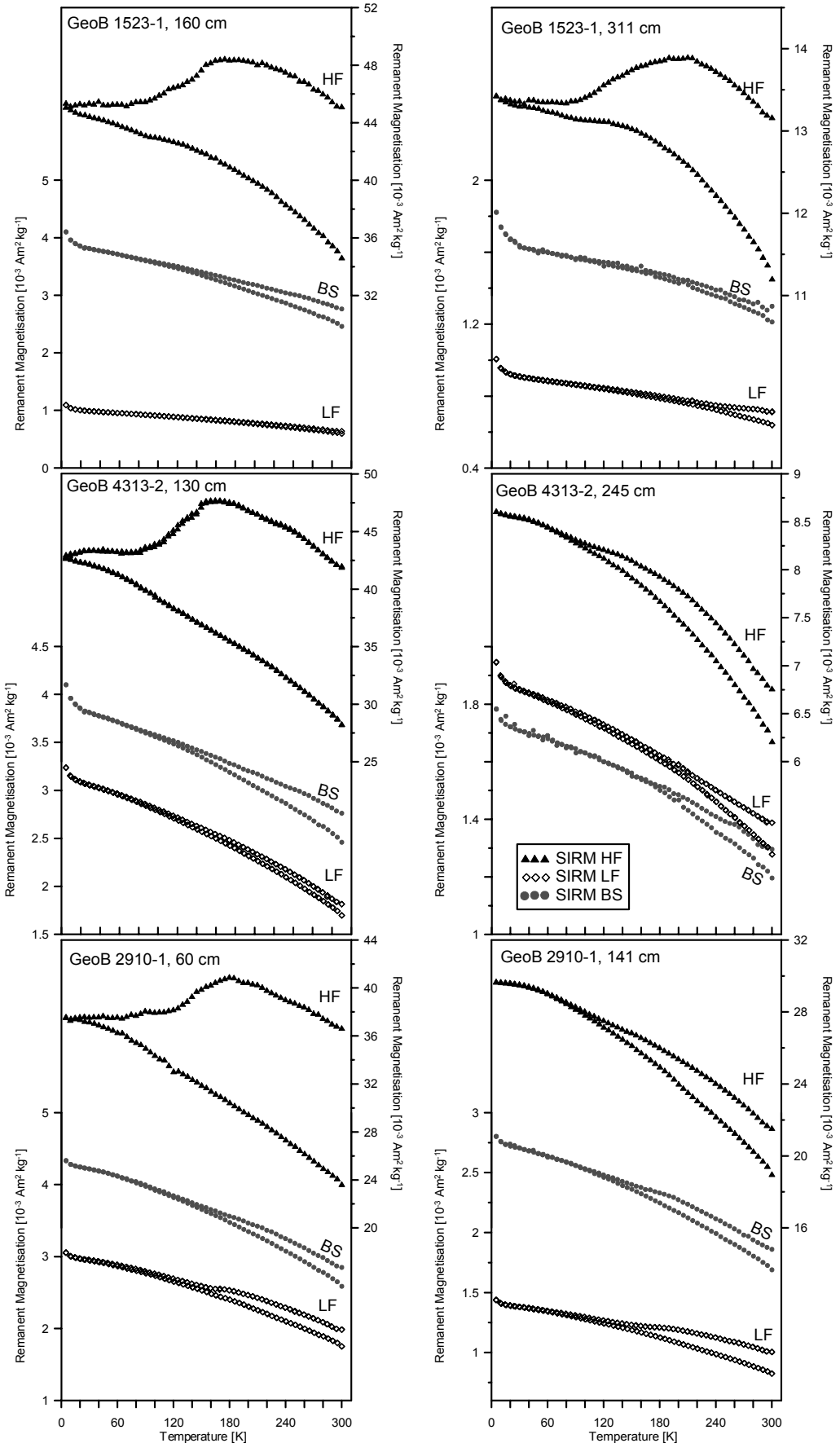
GeoB 1523-1, 160 cm
GeoB 1523-1, 311 cm
GeoB 4313-2, 130 cm
GeoB 4313-2, 245 cm
GeoB 2910-1, 60 cm
GeoB 2910-1, 141 cm
HF
BS
LF
SIRM HF
SIRM LF
SIRM BS
Remanent Magnetisation [10-3 Am2 kg-1]
Temperature [K]

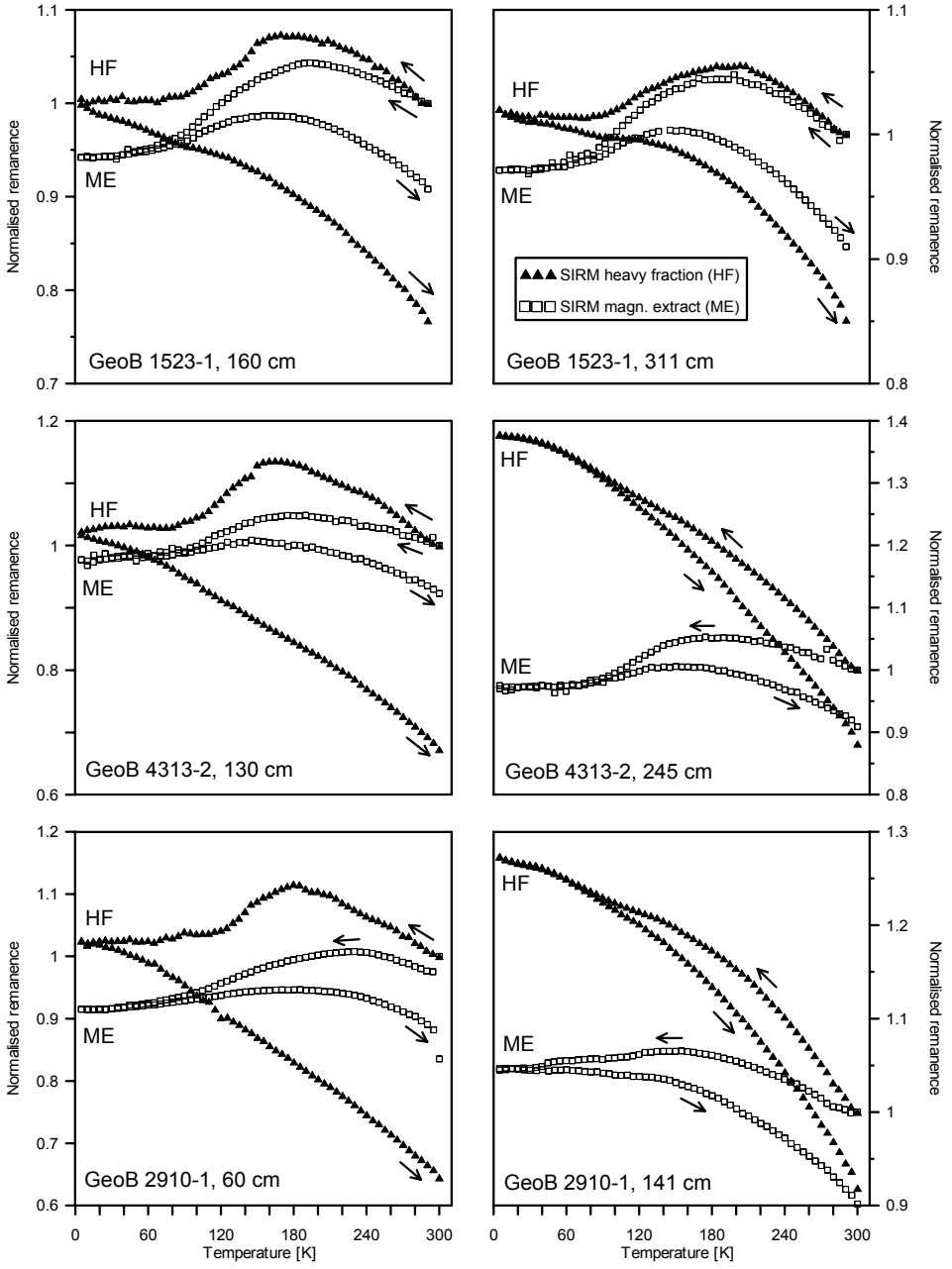

Figure 8. Comparisons of the zero-field cycles of RT-SIRM (applied field 5 T) for the heavy fractions (HF; black triangles) and the magnetic extracts (ME; open squares) of the six samples from a West to East profile (from top to bottom). ME curves are clearly dominated by the soft component magnetite, where as the HF curves show a steeper slope due to the high coercivity component goethite. Further detailed transitions in the temperature range between 240 and 180 K corresponding to the various present Fe-Ti phases. All ME and HF curves are normalised to the value of the respectively ZFC curve at 300 K as weight normalisation was not meaningful in case of the ME samples. The magnetically coarser samples from MIS 4 are shown in the left column and the magnetically finer samples from MIS 5.5 are shown in the right column.

Figure 7, page 37. Zero-field cycles of room temperature SIRM (applied field 5 T at 300 K) curves for the pristine dry bulk sediment samples (BS; gray dots), heavy fractions (HF; black triangles), and light fractions (LF; open diamonds) originating from the heavy liquid separation for the six samples from a West to East profile (from top to bottom). Samples from MIS 4 are shown on the left, samples from MIS 5.5 are shown on the right. The RT-SIRM curves were monitored in 2 K increments and normalised to their respectively sample mass. The BS and LF curves refer to the respective left ordinate axes, HF curves to the respective right ordinate axes. RT-SIRM curves of the HF show generally ten times higher remanence values than the BS samples, the LF curves show lower remanence values, except for sample GeoB 4313-2, 245 cm.

lutely complete and therefore we see a minor antiferromagnetic behaviour of the LF, strongly dominated by the paramagnetic components.

The RT-SIRM curves of the HF show characteristic low-temperature curves for (titano-) magnetite (Özdemir *et al*. 2002; Özdemir & Dunlop 2003; Kosterov 2003; Lagroix *et al*. 2004; Garming *et al*. in rev.), although we realise that RT-SIRM behaviour of (titano-) magnetites is not really well covered in the literature. Comparison of our HF curves with the titanomagnetite results from Özdemir & Dunlop (2003), Lagroix *et al.* (2004) and the RT-SIRM curves of Engelmann *et al*. (unpubl. data) from synthetic Fe-Ti oxide phases of various well defined Ti-content (Lattard *et al*. 2005) confirm the presence of (slightly oxidised) magnetite, various titanomagnetite, and titanohematite components in our samples.

Magnetic Extracts compared with Heavy Liquid Separates

Figure 8 shows the RT-SIRM curves of the magnetic extracts compared to the HF. For the sake of comparison, all curves were normalised to their value at 300 K. The RT-SIRM curves of the magnetic extracts clearly show ferrimagnetic dominated curves, typically of magnetite (Özdemir *et al.* 2002; Kosterov 2003). Comparing the differences between 125 and 105 K for both types of curves – the HF and the magnetic extracts – shows that magnetite is two times overrepresented in the latter. The cooling and warming curves are more or less reversible in the temperature range between 5 and 110 K. The relative changes of the remanence loss during the cooling-warming-cycle are only subtle. Generally samples from the westernmost sediment core show remanence losses of ~9%, the samples from the Mid-Atlantic Ridge site result in ~8% remanence loss and the easternmost samples have the biggest remanence losses of ~13%. The smooth increase with decreasing temperature, caused by the high coercivity component, is not present in the magnetic extract curves.

All RT-SIRM curves of the HF show this continuous increase with decreasing temperatures throughout the whole temperature range. This effect is attributed to the goethite component discussed before (Lowrie & Heller 1982, Dekkers 1989). The general shape of the RT-SIRM curves of the HF were already briefly described above. The occurrence of various Ti-Fe oxides is expressed by several minor changes of the cooling curve slope between 240 and 180 K. The undulations in the cooling curves above ~210 K should document the low-temperature magnetic ordering of present titanohematite phases (Lagroix *et al* 2004; Garming *et al*. in rev.), whereas the undulations detected on cooling below 210 K can be explained as magnetoelastical domain wall pinning postulated for this temperature range by Özdemir & Dunlop (2003). The RT-SIRM cycles of the MIS 5.5 samples of the cores GeoB 4313-2 and GeoB 2910-1 (Fig. 8) rather demonstrate characteristic curves for very Ti-rich oxide phases (Engelmann *et al*. unpubl. data) showing reversal behaviour in cooling and warming between 110 and 5 K. This is also expressed in the remanence loss behaviour of the HF samples: the westernmost sediment core GeoB 1523-1 shows remanence losses of ~13% for both samples, comparable to the remanence loss of ~12% for the MIS 5.5 samples from the Mid Atlantic Ridge (GeoB 4313-2) and the easternmost core (GeoB 2910-1). In contrast, the samples of MIS 4 from cores GeoB 4313-2 and GeoB 2910-1 have the biggest remanence loss of ~35%. This corresponds with findings of Özdemir et al. (2002), who describe an increasing remanence loss for stoichiometric magnetite of increasing grain-size.

5. Discussion

5.1 Further Magnetic Interpretations and Paleoclimatic Implications

The expression of the detected Verwey transition in the ZFC and FC curves of the

magnetic extract samples reflects the changing environmental conditions from West to East throughout the investigated transect in the Equatorial Atlantic. It is well known that the Verwey transition can be totally suppressed either by sufficient oxidation/maghemitisation (e.g. Özdemir *et al.* 1993) or by a fairly high Ti-content of $x \geq 0.4$ (e.g. Kakol *et al.* 1994) of the present magnetite ($Fe_{3-x}Ti_xO_4$). As already mentioned, additional SEM observations, using element dispersive spectroscopy (Goldstein *et al.* 1992), confirm the overall increase of the Ti-content in the magnetic mineral assemblage (Franke *et al.* unpubl. data). The Ti-content is exceedingly expressed by the shape of the RT-SIRM curves of the HF from GeoB 4313-2 and GeoB 2910-1 belonging to MIS 5.5. For the easternmost samples, supplementary Ti-rich titanohematite particles have been identified using electron backscatter diffraction techniques (Franke *et al*. in review). This suggests a (partial) dissolution of the original (titano-) magnetite particles with the concomitant increasing importance of the Ti-rich components, because the Ti-content stabilises the titanomagnetite compounds with regard to dissolution during diagenesis (Karlin 1990; Emiroğlu *et al.* 2004; Garming *et al*. 2005; Dillon & Bleil 2006).

The magnetic extracts do not contain much of a high coercivity component. Therefore they mainly represent the low-temperature behaviour of the low coercivity fraction in the magnetic assembly. The slightly steeper slope in ZFC and FC warming curves of the interglacial samples from MIS 5.5 indicates a finer magnetic grain-size of the low coercivity fraction compared to the glacial samples from MIS 4, which concurs with other magnetic grain-size observations in the dry bulk sediment measurements.

In the heavy liquid extraction procedure high coercivity components, such as goethite, were successfully extracted and contribute distinctly to the characteristics of the magnetic signal. In particular the RT-SIRM curves offer additional mineralogical and grain-size information, which was not detected by the LT-SIRM curves. Therefore low-temperature measurements on marine sediments using the heavy fraction might result in more detailed curves of more complete and quantitative samples. Comparison of the results from the MIS 4 and MIS 5.5 samples showed that the HF distinguished between their coarser and finer magnetic inventory and also showed a clear trend in dependence of the Ti-content of the magnetic assemblage. Funk *et al.* (2004a) described the magnetic grain-sizes of MIS 4 as much coarser as those of MIS 5.5. This does not concur with the reasoning of the coupling of the presence of an (enhanced) SP phase and the increased discrepancy of ZFC and FC curves. Another reasonable explanation of these ZFC and FC curve discrepancies was found in the temperature-dependent behaviour of goethite (Smirnov & Tarduno 2000).

5.2 Advantages of Heavy Liquid Separation

In the present study, we are dealing with natural samples of obviously complex composition and grain-size distributions and therefore our RT-SIRM curves are reflecting features of the various components. The absence in the HF measurements of the above mentioned ferrimagnetic ordering effect of paramagnetic material at very low temperatures confirms the success of the isolation of the dia- and paramagnetic fraction on the one hand and the ferrimagnetic and antiferromagnetic fraction on the other.

Comparisons of both extraction methods illustrate on the differences between the resulting samples. The magnetic extract exclusively represents the soft magnetic components of the dry bulk sediment. Within the range of soft magnetic components, magnetite certainly has the highest spontaneous magnetisation and is therefore preferably extracted by

methods such as described by Petersen *et al.* (1986) or Dekkers (1988). Additionally, the magnetic extraction leads generally to extracts that are coarser grained than the starting bulk sediment material.

Any sample upgrading technique can potentially alter the original material. For marine sediments from suboxic or anoxic environments, this could actually cause subsequent oxidation of iron sulphide mineral phases (e.g. greigite or pyrite). If the samples are suspended in a sediment slurry, the suspension should be deoxygenised by purging with an inert gas. This can be achieved by performing the upgrading in a closed cycle under argon atmosphere and the usage of alcohol instead of water as suspension medium.

In this study, we used non-toxic sodium polytungsten solution $Na_6[H_2W_{12}O_{40}]$. This heavy liquid does not react with the sample material and causes no additional oxidation. Its hydrophilic character allows us to disperse the relatively clay-rich homogenised dry bulk sediment reasonably well without usage of any additional peptiser. No chemical leaching had to be used, so the risk of alteration or even dissolution, particularly of the magnetic nanoparticles can be disregarded. The combination of heavy liquid separation, mechanical (and ultra-sonic) agitation and centrifuging accelerates the classical gravity separation method and leads generally to better results for marine sediment samples, avoiding clustering problems due to high clay content.

The light fraction always serves as a control measure for the success of the separation. Alternatively, as shown in Lagroix *et al* (2004), the specific density of the heavy liquid can be easily adjusted so that distinctly different magnetic fractions can be separated. In case of presence of paramagnetic heavy minerals, such as barite or siderite, these mineral phases are evidently included in the separated heavy fraction and have to be taken into account during low-temperature measurements (Frederichs *et al*. 2003).

The magnetic results for the heavy liquid separates presented here, confirm that the heavy fraction represents the complete range of the magnetic inventory to a reasonable extent. Using this technique, a much lager amount of magnetic material is available for measurements, which can be sufficiently quantified. As always, the success of the separation is generally depending on the grain-size distribution of the magnetic inventory. Especially components such as ultra-fine SP material are difficult to be completely extracted.

6. Conclusions

1. Magnetic extracts are not representative of the magnetic inventory in bulk sediment. Soft ferrimagnetic material is over-represented in the extract. Vice versa, much more weakly magnetic (antiferromagnetic) material, is under-represented. This has to be kept in mind during interpretation of the mineral magnetic data, e.g. low-temperature remanence curves.
2. Heavy liquid separation (with sodium polytungsten solution) is a useful tool to achieve a more complete 'magnetic' extract. It is as straightforward as magnetic extraction, both methods do not demand much experimental time. Heavy liquid separation allows the quantification of the resulting heavy and light mineral fractions and leads to larger yields of 'magnetic' extracts. Applied to fine-grained unconsolidated marine sediments, the combination of a hydrophile heavy liquid (polytungsten) dispersion with ultrasonic waves and subsequent centrifuging was very successful in separating the lighter dia- and paramagnetic mineral fraction from the heavy ferrimagnetic fraction. In sediments with appreciable non-ferrimagnetic heavy minerals, these will be included in the heavy liquid separate as well.
3. Comparison of the samples from MIS 4 and MIS 5.5 showed that the heavy liquid extraction improves in quality with increasing magnetic grain-size. However,

very fine material is still reasonably well extracted.
4. The RT-SIRM curves turned out to be the most indicative measurements for these marine sediment samples. Due to the variable Ti-content of the magnetite particles present those curves are more diagnostic in comparison to LT-ZFC and FC warming curves. Nevertheless, we recommend a combination of both remanence measurements for the sake of completeness and understanding of the low-temperature rock magnetic analysis.

Acknowlegements
The heavy liquid separation was performed at facilities of the Marine Geochemistry group, University of Bremen, we would like to thank particularly Michael Schweizer and Natascha Riedinger for their assistance. TC-Tungsten Compounds enterprises provided advice and heavy liquid solution for test runs. We also owe thanks to the members of the Marine Geophysics group (University of Bremen) and the Paleomagnetic group (Utrecht University) for their support and advice. Financial support of CF was provided by the DFG through the European Graduate College EUROPROX, (Universities of Bremen and Utrecht) and by NWO through the VMSG, Vening Meinesz Research School of Geodynamics (Utrecht University). This investigation is also associated to the Research Center Ocean Margins (RCOM) at the University of Bremen.

References

Coey, J.M.D., 1988. Magnetic properties of iron in soil iron oxides and clay minerals, in *Iron in Soils and Clay Minerals,* pp. 397-466, eds Stucki, J.W., Goodman, B.A. & Schwertmann, U., Reidel Publishing Company, Dortrecht.

Dekkers, M.J., 1988. *Some rockmagnetic parameters for natural goethite, pyrrhotite and fine-grained hematite*, Geologica Ultraiectina, **51**, Ph.D. thesis, Utrecht University, 231 p.

Dekkers, M.J., 1989. Magnetic properties of natural goethite - II. TRM behaviour during thermal and alternating field demagnetization and low-temperature treatment, *Geophys. J.*, **97**, 341-355.

Dillon, M. & Bleil, U., 2006. Rock Magnetic Signatures in Diagenetically Altered Sediments from the Niger Deep-Sea Fan, *J. Geophys. Res*., in press.

Emiroğlu, S., Rey, D. & Petersen, N., 2004. Magnetic properties of sediments in the Ría de Arousa (Spain): dissolution of iron oxides and formation of iron sulphides, *Phys. Chem. Earth*., **29**, 947-959.

Fischer, G. & cruise participants, 1998. Report and preliminary results of Meteor cruise M38/1, Las Palmas – Recife, 25.1.-1.3.1997, *Ber. Fachber. Geowiss. Univ. Bremen*, **94**, 178 p.

France, D.E. & Oldfield, F., 2000. Identifying goethite and hematite from rock magnetic measurements of soil and sediments, *J. Geophys. Res*., **105**, B2, 2781-2795.

Franke, C., Pennock, G.M., Drury, M.R., Lattard, D., Engelmann, R., Garming, J.F.L., von Dobeneck, T. & Dekkers, M.J., in review. Identification of magnetic Fe-Ti oxides by electron backscatter diffraction (EBSD) in scanning electron microscopy, *in review at J. Geophys. Res.*

Frederichs, T., von Dobeneck, T., Bleil, U. & Dekkers, M.J., 2003. Towards the identification of siderite, rhodochrostite and vivianite in sediments by their low-temperature magnetic properties, *Phys. Chem. Earth*, **28**, 669-679.

Funk, J., von Dobeneck, T. & Reitz, A., 2004a. Integrated rock magnetic and geochemical quantification of redoxomorphic iron mineral diagenesis in Late Quaternary sediments from the Equatorial Atlantic, in *The South Atlantic in the Late Quaternary: Reconstruction of Material Budget and Current Systems,* pp. 237-260, eds Wefer, G., Mulitza, S. & Ratmeyer, V., Springer-Verlag, Heidelberg, Berlin, New York.

Funk, J.A., von Dobeneck, T., Wagner, T. & Kasten, S., 2004b. Late Quaternary sedimentation and early diagenesis in the equatorial Atlantic Ocean: Patterns, trends and processes deduced from rock magnetic and geochemical records, in *The South Atlantic in the Late Quaternary: Reconstruction of Material Budget and Current Systems*, pp. 461-497, eds Wefer, G., Mulitza, S. & Ratmeyer, V., Springer-Verlag, Heidelberg, Berlin, New York.

Garming, J.F.L., Bleil, U. & Riedinger N., 2005. Alteration of magnetic mineralogy at the sulphate-methane transition: analysis of sediments from the Argentine continental slope, *Phys. Earth Planet. Inter*., **151**, 290-308.

Garming J.F.L., Bleil, U., Franke, C. & von Dobeneck, T., in review. Low-temperature partial magnetic self-reversal in marine sediments, *Geophys. J. Int.*

Goldstein, J.I., Newbury, D.E., Echlin, P., Joy, D.C., Romig, A.D.Jr., Lyman, C.E., Fiori, C. &

Lifshin, E., 1992. *Scanning electron microscopy and X-Ray microanalysis*, 2nd edition, Plenum Press, New York, 820p.

Hedley, I.G., 1971. The weak ferromagnetism of goethite (α-FeOOH), *Z. Geophy*., **37**, 409-420.

Heller, F., 1978. Rockmagnetic studies of Upper Jurassic limestones from Southern Germany, *J. Geophys*., **44**, 525-543.

Henrich, R. & cruise participants, 1994. Report and preliminary results of Meteor cruise M29/3, Rio de Janeiro - Las Palmas 11.8. - 5.9.1994. *Ber. Fachber. Geowiss. Univ. Bremen*, **60**, 155 p.

Hounslow, M.W. & Maher, B.A., 1999. Laboratory Procedures for Quantitavive Extraction and Analysis of Magnetic Minerals from Sediments, in *Environmental Magnetism, a practical guide*, pp. 139-164, eds Walden, J., Oldfield, F. & Smith, J., *Quaternary Research Association, Technical Guide,* **6**.

Kakol, Z., Sabol, J., Stickler, J., Kozlowski, A. & Honig, J.M., 1994. Influence of titanium doping on the magnetocrystalline anisotropy of magnetite, *Phys. Rev. B*, **49**, 12.767-12.772.

Karlin, R., 1990. Magnetic mineral diagenesis in suboxic sediments at Betis Site N-W, NE Pacific Ocean, *J. Geophys. Res*., **95**, 4421-4436.

Kosterov, A., 2003. Low-temperature magnetization and AC susceptibility of magnetite: effect of thermomagnetic history, *Geophys. J. Int*., **154**, 58-71.

Kosterov, A., Frederichs, T. & von Dobeneck, T., 2006. Low-temperature magnetic properties of rhodochrosite ($MnCO_3$), *Phys. Earth Planet. Inter.*, **154**, 234-242.

Lagroix, F., Banerjee, S.K. & Jackson, M.J., 2004. Magnetic properties of the Old Crow tephra: Identification of a complex iron titanium oxide mineralogy, *J. Geophys. Res*., 109, B01104, doi:10.1029/2003JB002678.

Lattard, D., Sauerzapf, U. & Käsemann, M., 2005. New calibration data for the Fe-Ti oxide thermo-oxybarometers from experiments in the Fe-Ti-O system at 1 bar, 1,000-1,300°C and a large range of oxygen fugacities, *Contrib. Mineral. Petrol*., **149**, 735-754.

Lowrie, W. & Heller, F., 1982. Magnetic properties of marine limestones, *Rev. Geophys. Space. Phys*., **20**, 171-192.

Özdemir, Ö., Dunlop, D.J. & Moskowitz, B.M., 1993. The effect of oxidation on the Verwey transition in magnetite, *Geophys. Res. Lett*., **20**, 1671-1674.

Özdemir, Ö. & Dunlop, D. J., 2000. Intermediate magnetite formation during dehydration of goethite, *Earth Planet. Sci. Lett*., **177**, 59-67.

Özdemir, Ö., Dunlop, D. & Moskowitz, B.M., 2002. Changes in remanence, coercivity and domain sate at low temperature in magnetite, *Earth Planet. Sci. Lett*., **194**, 343-358.

Özdemir, Ö. & Dunlop, D.J., 2003. Low-temperature behaviour and memory of iron-rich titanomagnetites (Mt. Haruna, Japan and Mt. Pinatubo, Philippines), *Earth Plant. Sci. Lett.*, **216**, 193-200.

Passier, H.F. & Dekkers, M.J., 2002. Iron oxide formation in the active oxidation front above sapropel S1 in the eastern Mediterranean Sea as derived from low-temperature magnetism, *Geophys. J. Int*., **150**, 230-240.

Petersen, H., von Dobeneck, T. & Vali, H., 1986. Fossil bacterial magnetite in deep-sea sediments from the South Atlantic Ocean, *Nature*, **320**, 611-615.

Reitz, A., Hensen, C., Kasten, S., Funk, J.A. & de Lange, G.J., 2004. A combined geochemical and rock-magnetic investigation of a redox horizon at the last glacial/interglacial transition, *Phys. Chem. Earth*, **29**, 921-931.

Smirnov, A.V. & Tarduno, J.A., 2000. Low-temperature magnetic properties of pelagic sediments (Ocean Drilling Program Site 805C): Tracers of maghemitization and magnetic mineral reduction, *J. Geophys. Res*., **107**, B7, 16457-16471.

Schulz, H.D. & cruise participants, 1991. Report and preliminary results of Meteor cruise M16/2, Recife – Belem, 28.4.-20.5.1991, *Ber. Fachber. Geowiss. Univ. Bremen,* **19**, 149 p.

Van Velzen, A.J. & Zijderveld, J.D.A., 1992. A method to study alterations of magnetic minerals during thermal demagnetization applied to a fine-grained marine marl (Trubi Formation, Sicily), *Geophys. J. Int*., **110**, 79-90.

Van Velzen, A.J. & Zijderveld, J.D.A., 1995. Effects of weathering on single domain magnetite in early Pliocene marls, *Geophys. J. Int*., **121**, 267-278.

Van Velzen A.J. & Dekkers M.J., 1999a. Low-temperature oxidation of magnetite in loess-paleosol sequences: a correction of rock magnetic parameters, *Studia Geophysica et Geodaetica*, **43**, 4, 357-375.

Van Velzen, A.J. & Dekkers, M.J., 1999b. The incorporation of thermal methods in mineral magnetism of loess-paleosol sequences: a brief overview, *Chin. Sci. Bull*., **44**, Suppl. 1, 53-63.

von Dobeneck, T., Petersen, N. & Vali, H., 1987. Bakterielle Magnetofossilien – paläomagnetische und paläontologische Spuren einer ungewöhnlichen Bakteriengruppe, *Geowissenschaften in unserer Zeit*, **1**, 27-35.